

Dynamically assisted interlayer hopping in $\text{YBa}_2\text{Cu}_3\text{O}_{6+x}$

P. Nyhus, M. A. Karlow, and S. L. Cooper

Department of Physics and Frederick Seitz Materials Research Laboratory, University of Illinois at Urbana-Champaign, Urbana, Illinois 61801

B. W. Veal and A. P. Paulikas

Materials Science Division, Argonne National Laboratory, Argonne, Illinois 60439

(Received 18 May 1994)

We report evidence from c -axis-polarized Raman scattering and optical-reflectivity measurements that doping-induced and phonon-mediated changes in the O(4)-Cu(1)-O(4) structure influence c -axis charge dynamics in $\text{YBa}_2\text{Cu}_3\text{O}_{6+x}$. With increased doping, we observe a rapid increase in the interbilayer hopping rate which we suggest may be caused by the systematic decrease in the Cu(2)-O(4) bond length. Also, c -axis-polarized Raman scattering measurements provide evidence that dynamical modulation of the O(4)-Cu(2) bond length by c -axis phonons contributes to "assisted" interbilayer hopping.

In spite of increased experimental and theoretical study, there are many unresolved issues concerning c -axis charge transport in the layered high- T_c cuprates. For example, the measured resistivity anisotropies of the cuprates are substantially larger [$\rho_c/\rho_{ab} \sim 10^2-10^5$ (Ref. 1)] than band-structure estimates [$\rho_c/\rho_{ab} \sim 10$ (Ref. 2)], suggesting that one must go beyond the Bloch-Boltzmann model to understand the mechanism constraining the interlayer hopping rate in these materials. Additionally, band-structure calculations predict that the cuprates should exhibit metallic c -axis resistivities ($d\rho_c/dT > 0$),² yet the c -axis resistivities in most of the layered cuprates have a semiconductorlike temperature dependence (i.e., $d\rho_c/dT < 0$) at low temperatures. Finally, both $\text{YBa}_2\text{Cu}_3\text{O}_{6+x}$ and $\text{La}_{2-x}\text{Sr}_x\text{CuO}_4$ have a doping-dependent anisotropy that is not yet well understood.^{1,3} A number of models have been proposed to address one or more of these unusual transport features, including anisotropic localization,^{4,5} interlayer tunneling between certain non-Fermi liquids,^{6,7} and "assisted" interlayer scattering from impurities⁸ or bosons.⁹ Unfortunately, there is as yet no definitive evidence in favor of any of these models.

In this paper, we report Raman scattering and optical reflectivity studies of the mechanisms contributing to c -axis charge transport in $\text{YBa}_2\text{Cu}_3\text{O}_{6+x}$. Our results suggest that the O(4)-Cu(1)-O(4) structure between the CuO bilayers plays an important role in governing the doping and temperature dependence of the interbilayer hopping rate in $\text{YBa}_2\text{Cu}_3\text{O}_{6+x}$. For example, we find evidence that the interbilayer coupling integral varies roughly exponentially with doping, which we attribute to doping-induced changes in the Cu(2)-O(4) bond length. Moreover, our Raman results suggest that the 500 cm^{-1} c -axis O(4) phonon, and possibly other c -axis phonons, contribute to phonon-assisted interlayer hopping in $\text{YBa}_2\text{Cu}_3\text{O}_{6+x}$. This is direct evidence of a specific *incoherent* contribution to c -axis transport in the cuprates.

Raman and optical reflectivity spectra were obtained on a series of thick (0.2–0.75 mm in the c direction) $\text{YBa}_2\text{Cu}_3\text{O}_{6+x}$ samples with oxygen concentrations $x \sim 0.93$ ($T_c \sim 90\text{ K}$), $x \sim 0.85$ ($T_c \sim 93\text{ K}$), $x \sim 0.75$ ($T_c \sim 80\text{ K}$),

$x \sim 0.65$ ($T_c \sim 60\text{ K}$), $x \sim 0.50$ ($T_c \sim 50\text{ K}$), $x \sim 0.41$ ($T_c \sim 30\text{ K}$), $x \sim 0.37$ ($T_c \sim 15\text{ K}$), and $x \sim 0.30, 0.25, 0.10$ ($T_c \sim 0\text{ K}$). The Raman spectra were taken in a pseudobackscattering geometry with 5145 or 4579 \AA laser light polarized along the c -axis direction. All Raman spectra were corrected for the frequency-dependent response of the system and for the optical responses of the materials. Optical reflectivity measurements with light polarized along the c -axis direction were obtained between 125 and 16000 cm^{-1} using a rapid-scanning Fourier transform interferometer in a near-normal incidence geometry.

Figure 1 shows the c -axis-polarized [$(\mathbf{E}_i, \mathbf{E}_s) = (z, z)$] high-frequency Raman spectrum as a function of doping. The c -axis polarized spectra exhibit a strong electronic continuum with a $1/\omega$ frequency dependence at high frequencies,³ as well as the two-phonon overtone of the 500

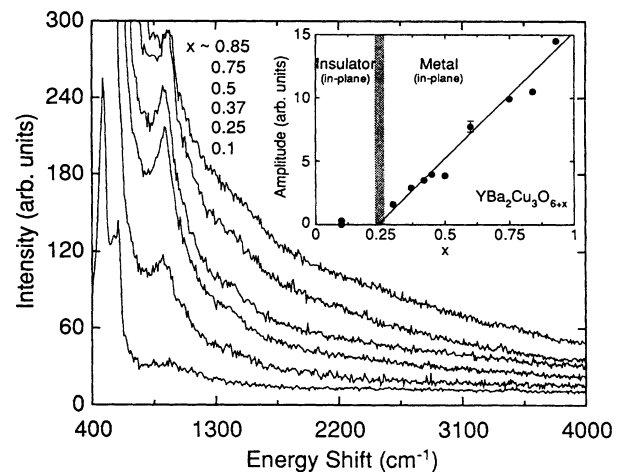


FIG. 1. Room-temperature c -axis-polarized [$(\mathbf{E}_i, \mathbf{E}_s) = (z, z)$] Raman continuum above 500 cm^{-1} for several doping levels of $\text{YBa}_2\text{Cu}_3\text{O}_{6+x}$ (top to bottom) $x = 0.85, 0.75, 0.50, 0.37, 0.25, 0.10$. The inset shows the amplitude of continuum scattering, A , as a function of doping, x . The error bar reflects the uncertainty in establishing the zero of continuum scattering intensity.

cm^{-1} c -axis O(4) mode. As shown in the inset of Fig. 1, the continuum scattering amplitude scales with the in-plane carrier density, decreasing roughly linearly with decreased doping and disappearing below the in-plane metal-insulator transition (inset, Fig. 1). By contrast, all depolarized (z,x) spectra are featureless, indicating that the c -axis electronic continuum is strongly (z,z) polarized.

The strong, high-frequency c -axis Raman continuum in $\text{YBa}_2\text{Cu}_3\text{O}_{6+x}$ cannot result from isotropic ($L=0$) charge-density fluctuations, as these are screened by the long-range Coulomb interaction, and have a weak Raman scattering response with a low characteristic energy, qv_F , where q is the wave vector of the light and v_F is the Fermi velocity. However, in anisotropic systems such as the layered cuprates, density fluctuations associated with different parts of the Fermi surface ($L \neq 0$) are not screened, and can give strong Raman scattering intensities and large Raman shifts when,¹⁰ (i) there is a large effective mass difference between the initial and final states in the scattering process, and (ii) there is impurity or phonon scattering to conserve crystal momentum in the scattering process. For example, strong electronic Raman scattering has been observed for “intervalley” electronic scattering between longitudinal and transverse portions of the multivalley Fermi surface in n -type Si, with impurity scattering providing crystal momentum conservation.¹¹ Notably, conditions (i) and (ii) imply that impurity- or boson-assisted hopping contributions to interlayer transport should have strong Raman scattering intensities in anisotropic systems such as the cuprates.

Combined with estimates of the c -axis plasma frequency,¹ the extremely large scattering rate ($\Gamma \sim 1000 \text{ cm}^{-1}$ in $\text{YBa}_2\text{Cu}_3\text{O}_7$) associated with the c -axis continuum in $\text{YBa}_2\text{Cu}_3\text{O}_{6+x}$ is consistent with interlayer scattering in a very “dirty” metal, with scattering occurring nearly every unit cell. While static impurities are a possible source of this scattering, Raman scattering in a dirty metal is characterized by a collision-dominated response function,¹⁰ $\text{Im}R(\omega) = A\omega\Gamma/(\omega^2 + \Gamma^2)$, which clearly does not fit the low-temperature Raman spectrum in Fig. 2 (dotted line). Rather, Fig. 2 suggests that the c -axis continuum in $\text{YBa}_2\text{Cu}_3\text{O}_{6+x}$ is more appropriately associated with interlayer scattering via emission of c -axis optical phonons. For example, the doping dependence of the (zz) Raman spectrum (inset of Fig. 2) shows that the c -axis continuum turns on abruptly above the 500 cm^{-1} O(4) phonon frequency, suggesting that the 500 cm^{-1} optical phonon, which is a c -axis vibration of the apical O(4) atom between the Cu(1) chain and Cu(2) plane sites, is emitted in the c -axis continuum scattering process. By contrast, scattering from impurities or acoustic phonons would be characterized by an electronic continuum extending to arbitrarily low energies. Itai¹² has shown that Raman scattering from electron-hole pairs with the emission of an Einstein phonon has the signature of a collision-dominated response function that is *shifted* by the energy of the Einstein phonon. Such a response is seen in Fig. 2, which illustrates that the 5 K c -axis Raman spectrum of $\text{YBa}_2\text{Cu}_3\text{O}_{6+x}$ can be nicely fit with a collision-dominated response function ($\Gamma \sim 1000 \text{ cm}^{-1}$) that is shifted by the 500 cm^{-1} phonon frequency ω_0 (dashed line). These results provide strong evidence that the c -axis continuum involves phonon-assisted interlayer scattering, with the 500 cm^{-1}

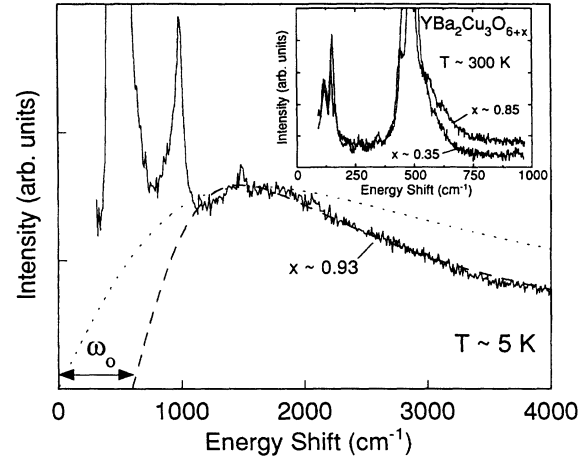


FIG. 2. c -axis-polarized [$(\mathbf{E}_i, \mathbf{E}_s) = (z, z)$] Raman continuum for $x=0.93$ at 5 K. The dashed line is a fit of the continuum to a collision-dominated response function, $\text{Im}R(\omega) = A\omega\Gamma/(\omega^2 + \Gamma^2)$, which has been *shifted* by an optical phonon frequency, $\omega_0 \sim 500 \text{ cm}^{-1}$, as described in a model by Itai described in the text (Ref. 13). The dotted line compares the best fit using an unshifted collision-dominated response function. The inset shows the doping dependence of the low-frequency (z,z) Raman response, illustrating the abrupt onset of c -axis continuum scattering above the $\omega_0 = 500 \text{ cm}^{-1}$ O(4) phonon energy.

c -axis O(4) phonon supplying the momentum transfer necessary to scatter carriers from their initial in-plane momentum states to adjacent bilayers,¹³ and with the large effective mass differences between in-plane and out-of-plane initial and final states¹⁴ contributing to the strong Raman scattering intensity.

The evidence for phonon-assisted interlayer scattering in $\text{YBa}_2\text{Cu}_3\text{O}_{6+x}$ given above is the first identification of a specific incoherent contribution to c -axis transport in the cuprates. The importance of incoherent contributions to c -axis transport in the cuprates has been discussed by several groups, all of whom suggest a phenomenological expression for the c -axis resistivity:^{9,15,16}

$$\rho_c(T) \sim AT + B/T, \quad (1)$$

where the first term represents a metallic (coherent) contribution, and the second term reflects various incoherent contributions. Rojo and Levin⁹ in particular have suggested that c -axis phonons may provide an important incoherent hopping mechanism in the cuprates. Littlewood and Varma¹⁵ argue that c -axis transport in the cuprates is intrinsically metallic [i.e., $B=0$ in Eq. (1)], but that an incoherent contribution to c -axis transport is possible due to the breaking of momentum conservation by impurities in the spacer layer between CuO cells (i.e., bilayer, trilayers, etc.). Significantly, our results suggest that vibrational modes associated with the spacer layer, such as the 500 cm^{-1} O(4) mode, can provide an *intrinsic* source of incoherent interlayer hopping in $\text{YBa}_2\text{Cu}_3\text{O}_{6+x}$.

A limitation of Eq. (1) as a phenomenological description of the c -axis resistivity in $\text{YBa}_2\text{Cu}_3\text{O}_{6+x}$ is that it does not naturally describe the doping-dependence of either $\rho_c(T)$ or the effective c -axis plasma frequency ω_{pc} . For example,

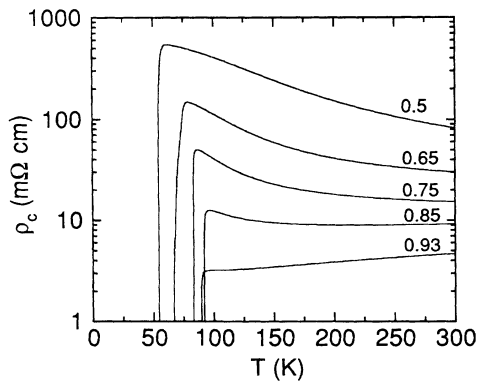


FIG. 3. Temperature- and doping-dependent c -axis resistivity for $\text{YBa}_2\text{Cu}_3\text{O}_{6+x}$, illustrating the roughly exponential doping dependence, and the semiconductorlike low-temperature upturn for oxygen-deficient samples. Doping levels, x , are listed above the resistivity curves.

Fig. 3 presents the temperature and doping dependence of ρ_c for our $\text{YBa}_2\text{Cu}_3\text{O}_{6+x}$ samples, illustrating that in addition to a semiconductorlike low-temperature resistivity in all but the most highly doped sample, $\rho_c(T)$ exhibits a roughly exponential doping dependence throughout the temperature range. Also, Fig. 4 shows the c -axis reflectivity of $\text{YBa}_2\text{Cu}_3\text{O}_{6+x}$ as a function of doping, from which we have determined $\sigma_c(\omega)$ and the electronic contribution to the integrated c -axis spectral weight, $N_{\text{eff}}^c(\omega') = (2mV/\pi e^2) \int_0^{\omega'} \sigma_c^{(e)}(\omega) d\omega$, where m , e , and V are the bare electron mass, electronic charge, and unit cell volume, respectively, and where $\sigma_c^{(e)}(\omega)$ is obtained by subtracting the phonons from the c -axis conductivity, $\sigma_c(\omega)$. The inset of Fig. 4 plots the doping dependence of $N_{\text{eff}}^c(\omega' = 0.2 \text{ eV})$. $N_{\text{eff}}^c(0.2 \text{ eV})$ provides a reasonable estimate of the spectral weight associated with the low-frequency electronic contribution to $\sigma_c(\omega)$, and is related to a squared equivalent c -axis plasma frequency by $\omega_{pc}^2 (eV^2) = 8N_{\text{eff}}^c$. In materials with an open Fermi surface such as the cuprates, the c -axis plasma

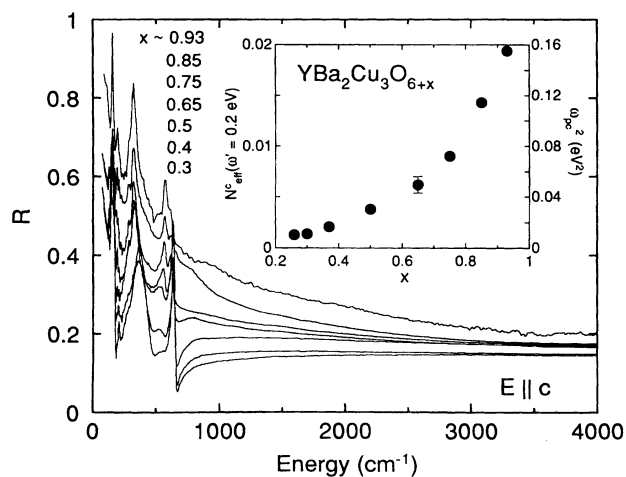


FIG. 4. Reflectance for light polarized along c axis for several doping levels. Inset shows the doping dependence of $N_{\text{eff}}^c(0.2 \text{ eV})$ obtained from the c -axis reflectivities of $\text{YBa}_2\text{Cu}_3\text{O}_{6+x}$.

frequency provides an estimate of the interbilayer coupling integral:^{1,17} $\omega_{pc}/\omega_{pab} \sim (c/a)(t_c/E')$, where ω_{pc} and ω_{pab} are the c -axis and in-plane plasma frequencies, respectively, c and a are the c -axis and in-plane lattice parameters, respectively, E' is related to the in-plane Fermi velocity, and t_c is the interlayer coupling integral. The inset of Fig. 4 illustrates that $N_{\text{eff}}^c(0.2 \text{ eV})$ in $\text{YBa}_2\text{Cu}_3\text{O}_{6+x}$ is small at low doping, but increases rapidly with x . Indeed, the ρ_c and N_{eff}^c data in Figs. 3 and 4 suggest that the doping dependence of the interbilayer coupling integral in $\text{YBa}_2\text{Cu}_3\text{O}_{6+x}$ can be approximately described by $t_c \sim \exp[-\alpha d(x)]$, where α is a constant and $d(x)$ is an effective barrier width that varies roughly linearly with doping.

The nature of the barrier in $\text{YBa}_2\text{Cu}_3\text{O}_{6+x}$, and the possible origin of the strong doping dependencies of ρ_c and N_{eff}^c , are suggested by evidence that intercell coupling in $\text{YBa}_2\text{Cu}_3\text{O}_{6+x}$ and $\text{La}_{2-x}\text{Sr}_x\text{CuO}_4$ is sensitive to the hybridization between apical O p_z states and in-plane Cu states. For example, x-ray absorption measurements of $\text{La}_{2-x}\text{Sr}_x\text{CuO}_4$ by Chen *et al.*¹⁸ suggest that increased interlayer coupling with doping arises from a systematic increase in the contribution of the apical O p_z orbital to the doped holes. In $\text{YBa}_2\text{Cu}_3\text{O}_{6+x}$, resonance Raman scattering experiments also show evidence for increased admixing of O(4) p_z and in-plane states as doping is increased.¹⁹ Finally, neutron-diffraction measurements of $\text{YBa}_2\text{Cu}_3\text{O}_{6+x}$ by Jorgensen *et al.*²⁰ show that there is a quasilinear decrease in the O(4)-Cu(2) bond length with increased doping, suggesting a mechanism by which a systematic increase in O(4) $p_z/\text{Cu}(2) d_{3z^2-1}$ hybridization, and a concomitant increase in interbilayer coupling, can occur with doping.

The possibility that interbilayer coupling in $\text{YBa}_2\text{Cu}_3\text{O}_{6+x}$ is sensitive to hybridization between O(4) p_z and Cu(2) d_{3z^2-1} states is particularly interesting given our evidence that the 500 cm^{-1} apical O(4) phonon contributes to phonon-assisted interbilayer hopping, as it is known that this mode strongly modulates the overlap integral associated with both the O(4)-Cu(2) and O(4)-Cu(1) bonds.¹⁹ This suggests that the 500 cm^{-1} apical O(4) mode, as well as other c -axis phonons, may influence c -axis transport in $\text{YBa}_2\text{Cu}_3\text{O}_{6+x}$ by dynamically modulating the interlayer hopping rate. Renormalization of interlayer hopping by slow boson degrees of freedom is possible in anisotropic materials such as $\text{YBa}_2\text{Cu}_3\text{O}_{6+x}$ and $\text{La}_{2-x}\text{Sr}_x\text{CuO}_4$ because the weak intercell hopping rates are on the order of phonon energies. Kumar and Jayannavar⁴ suggested that c -axis phonons might renormalize the interlayer hopping rate in the cuprates, and thereby cause semiconductorlike resistivities at low temperatures, motivated by analogies with adiabatic renormalization of the tunneling matrix element by bosons in two-level systems.²¹ Notably, evidence that the c -axis O(4) mode contributes to assisted interlayer hopping suggests that c -axis acoustic phonons should also effectively modulate the interbilayer hopping rate. Raman scattering from electron-hole pairs with *acoustic* phonon emission would be evident as an electronic continuum that extends to zero energy,¹² and Mihailovic, McCarty, and Ginley²² have indeed observed a flat, low-frequency c -axis continuum in $\text{YBa}_2\text{Cu}_3\text{O}_7$ that has a temperature dependence consistent with a two-particle emission process.

A simple description of interlayer transport in which the interlayer hopping rate is modulated by phonons or other bosons provides a possible description of the temperature and doping dependence of ρ_c in $\text{YBa}_2\text{Cu}_3\text{O}_{6+x}$ (see Fig. 3). Taking the interbilayer coupling integral to be $t_c = t_{c0} \exp(-\alpha d)$, where t_{c0} is the static coupling integral, α is a constant, $d = d_0(1 + \delta)$ is the instantaneous barrier width, d_0 is the equilibrium width, and $\delta(T)$ is the fractional change in the barrier width due to c -axis phonons, then for small $\delta(T)$, the interbilayer coupling integral is given roughly as $t_c(T) \sim t_{c0} \exp(-\alpha d_0) \{1 - \alpha d_0 \delta(T)\}$, where the first term represents direct (coherent) hopping, and the second term represents the dynamical modulation of t_c by bosons. This simple picture qualitatively describes several important aspects of the c -axis reflectivity (Fig. 4) and resistivity (Fig. 3) of $\text{YBa}_2\text{Cu}_3\text{O}_{6+x}$. First, the doping dependence of t_c is dominated by rapid changes in the static coupling integral, $t_{c0} \exp(-\alpha d_0)$, which we have argued result from the systematic decrease of the O(4)-Cu(2) bond length with doping observed by Jorgensen *et al.*¹⁹ The second term associated with boson-modulation of the interbilayer coupling integral contributes a semiconductinglike temperature

dependence to $\rho_c(T)$, due to the decreasing population of phonons or other bosons at low temperatures. Finally, this picture suggests that the decreasing size of the semiconductorlike upturn in $\rho_c(T)$ with increased doping (Fig. 3) may arise because there is a decreased relative contribution of assisted hopping to the total c -axis conductivity as interbilayer coupling increases.

To summarize, our results suggest that interlayer hopping in $\text{YBa}_2\text{Cu}_3\text{O}_{6+x}$ is influenced both by doping-induced structural changes in the Cu(2)-O(4) bond length, and by phonon-assisted hopping. An important issue which has not been addressed concerns the small size of the hopping rate in the cuprates relative to band-structure predictions. Future studies are necessary to investigate mechanisms by which the interlayer hopping rate might be renormalized in the layered cuprates, including mechanisms involving interlayer tunneling^{6,7} dynamically detuned hopping,²³ and the renormalization of hopping by impurity scattering.⁴

This work was supported by NSF DMR91-20000 through the Science and Technology Center for Superconductivity (P.N., M.A.K., and S.L.C.) and by the Department of Energy through W-31-109-Eng-33 (B.W.V. and A.P.P.).

¹S. L. Cooper and K. E. Gray, in *Physical Properties of High Temperature Superconductors IV*, edited by D. M. Ginsberg (World Scientific, Singapore, 1994), and references therein.

²W. E. Pickett, *Rev. Mod. Phys.* **61**, 433 (1989).

³S. L. Cooper, P. Nyhus, D. Reznik, M. V. Klein, W. C. Lee, D. M. Ginsberg, B. W. Veal, A. P. Paulikas, and B. Dabrowski, *Phys. Rev. Lett.* **70**, 1533 (1993).

⁴N. Kumar and A. M. Jayannavar, *Phys. Rev. B* **45**, 5001 (1992).

⁵G. Kotliar, E. Abrahams, A. E. Ruckenstein, C. M. Varma, P. B. Littlewood, and S. Schmitt-Rink, *Europhys. Lett.* **15**, 655 (1991).

⁶S. Chakravarty, A. Sudbo, P. W. Anderson, and S. Strong, *Science* **261**, 337 (1993).

⁷P. W. Anderson, *Science* **256**, 1526 (1992).

⁸M. J. Graf, D. Rainer, and J. A. Sauls, *Phys. Rev. B* **47**, 12 089 (1993).

⁹A. G. Rojo and K. Levin, *Phys. Rev. B* **48**, 16 861 (1993).

¹⁰J. Kosztin and A. Zawadowski, *Solid State Commun.* **78**, 1029 (1991); A. Zawadowski and M. Cardona, *Phys. Rev. B* **42**, 10 732 (1990).

¹¹G. Contreras, A. K. Sood, and M. Cardona, *Phys. Rev. B* **32**, 924 (1985).

¹²K. Itai, *Phys. Rev. B* **45**, 707 (1992).

¹³In this respect, the O(4) phonon plays a role similar to that attributed to the spins in c -axis tunneling, see J. R. Kirtley and D. J. Scalapino, *Phys. Rev. Lett.* **65**, 798 (1990).

¹⁴It is also possible the effective mass difference between CuO plane and chain layers contributes to the scattering intensity.

¹⁵P. B. Littlewood and C. M. Varma, *Phys. Rev. B* **45**, 12 636 (1992).

¹⁶P. W. Anderson and Z. Zou, *Phys. Rev. Lett.* **60**, 132 (1988).

¹⁷V. Zelezny, D. B. Tanner, K. Kamaras, L. P. Kozeeva, and A. A. Pavlyuk (unpublished).

¹⁸C. T. Chen, L. H. Tjeng, J. Kwo, H. L. Kao, P. Rudolf, F. Sette, and R. M. Flemming, *Phys. Rev. Lett.* **68**, 2543 (1992).

¹⁹E. T. Heyen, J. Kircher, and M. Cardona, *Phys. Rev. B* **45**, 3037 (1992); E. T. Heyen, S. N. Rashkeev, I. I. Mazin, O. K. Andersen, R. Liu, M. Cardona, and O. Jepsen, *Phys. Rev. Lett.* **65**, 3048 (1990).

²⁰J. D. Jorgensen, B. W. Veal, A. P. Paulikas, L. J. Nowicki, G. W. Crabtree, H. Claus, and W. K. Kwok, *Phys. Rev. B* **41**, 1863 (1990).

²¹A. J. Leggett, S. Chakravarty, A. T. Dorsey, M. P. A. Fisher, A. Garg, and W. Zwerger, *Rev. Mod. Phys.* **59**, 1 (1987).

²²D. Mihailovic, K. F. McCarty, and D. S. Ginley, *Phys. Rev. B* **47**, 8910 (1993).

²³A. J. Leggett, *Braz. J. Phys.* **22**, 129 (1992).

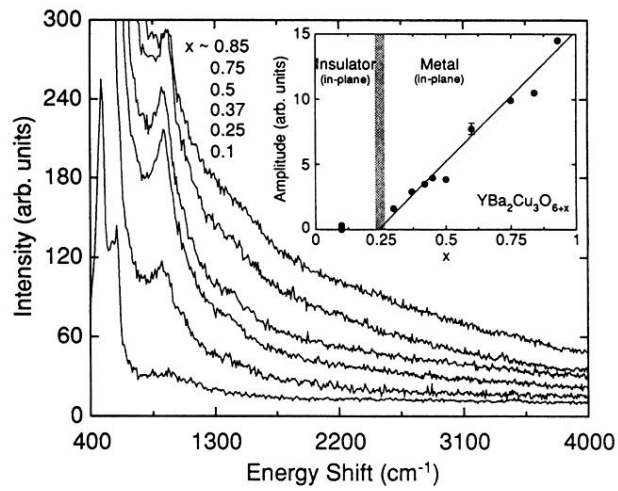


FIG. 1. Room-temperature c -axis-polarized $[(\mathbf{E}_i, \mathbf{E}_s) = (z, z)]$ Raman continuum above 500 cm^{-1} for several doping levels of $\text{YBa}_2\text{Cu}_3\text{O}_{6+x}$ (top to bottom) $x = 0.85, 0.75, 0.50, 0.37, 0.25, 0.10$. The inset shows the amplitude of continuum scattering, A , as a function of doping, x . The error bar reflects the uncertainty in establishing the zero of continuum scattering intensity.